

$$\mathbf{v}_{\theta g} = \frac{1}{2}(\mathbf{c}_\theta - fr) + \left[\left(\frac{\mathbf{c}_\theta - fr}{2} \right)^2 + \frac{r}{\rho} \frac{\partial \mathbf{P}}{\partial r} \right]^{1/2} \quad (15)$$

The radial velocity \mathbf{v}_{rg} can be obtained from continuity equation as

$$\mathbf{v}_{rg} = -\frac{1}{r} \int_0^r \frac{\partial \mathbf{v}_{\theta g}}{\partial \theta} dr \quad (16)$$

In the study, \mathbf{v}_{rg} is set at 0.

In the analysis, \mathbf{v}' is assumed much smaller than \mathbf{v}_g , and the first derivative of the velocity components \mathbf{v}'_θ , \mathbf{v}'_r with respect to θ are much smaller compared with the velocity components. Then, equation (9) can be linearized as follows,

$$-\left(2 \frac{\mathbf{v}_{\theta g}}{r} + f \right) \mathbf{v}'_\theta = k_m \frac{\partial^2 \mathbf{v}'_r}{\partial z^2} \quad (17)$$

$$\left(\frac{\partial \mathbf{v}_{\theta g}}{\partial r} + \frac{\mathbf{v}_{\theta g}}{r} + f \right) \mathbf{v}'_r = k_m \frac{\partial^2 \mathbf{v}'_\theta}{\partial z^2} \quad (18)$$

Introducing the following two abbreviations,

$$\xi = \left(\frac{\partial \mathbf{v}_{\theta g}}{\partial r} + \frac{\mathbf{v}_{\theta g}}{r} + f \right)^{1/2} / \left(2\mathbf{v}_{\theta g}/r + f \right)^{1/2} \quad (19)$$

$$\lambda = \left(\frac{\partial \mathbf{v}_{\theta g}}{\partial r} + \frac{\mathbf{v}_{\theta g}}{r} + f \right)^{1/4} \left(2 \frac{\mathbf{v}_{\theta g}}{r} + f \right)^{1/4} / (2k_m)^{1/2} \quad (20)$$

And equations (17) and (18) becomes

$$2\lambda^2 \mathbf{v}''_\theta = \frac{\partial^2 \mathbf{v}''_r}{\partial z^2} \quad (21)$$

$$-2\lambda^2 \mathbf{v}''_r = \frac{\partial^2 \mathbf{v}''_\theta}{\partial z^2} \quad (22)$$

Where $\mathbf{v}''_\theta = \mathbf{v}'_\theta$ and $\mathbf{v}''_r = -\mathbf{v}'_r/\xi$. Equation (21) times i and adds equation (22) then got the following equation

$$\frac{\partial^2 \mathbf{v}''}{\partial z^2} - [(1+i)\lambda]^2 \mathbf{v}'' = 0 \quad (23)$$

Considering boundary condition of equation (10), solution can be obtained as

$$\mathbf{v}'' = \mathbf{D} \exp[-(1+i)\lambda z'] \quad (24)$$

Where $\mathbf{D} = \mathbf{D}_1 + i\mathbf{D}_2$ is a complex constant. The velocity components in the boundary layer are obtained as

$$\mathbf{v}'_\theta = e^{-\lambda z'} [\mathbf{D}_1 \cos(\lambda z') + \mathbf{D}_2 \sin(\lambda z')] \quad (25)$$

$$\mathbf{v}'_r = -\xi e^{-\lambda z'} [\mathbf{D}_2 \cos(\lambda z') - \mathbf{D}_1 \sin(\lambda z')] \quad (26)$$

Where

$$D_1 = -\frac{\chi(\chi+1)\mathbf{v}_{\theta g} - \chi\mathbf{v}_{rg}/\xi}{1+(\chi+1)^2}$$

$$D_2 = \frac{\chi\mathbf{v}_{\theta g} + \chi(\chi+1)\mathbf{v}_{rg}/\xi}{1+(\chi+1)^2}$$

$$\chi = \frac{C_d}{k_m \lambda} |\mathbf{v}_s| = \frac{C_d}{k_m \lambda} \sqrt{\mathbf{v}_{\theta s}^2 + \mathbf{v}_{\theta r}^2}$$

3. RADIUS OF MAXIMUM WIND VELOCITY R_{\max} AND RADIAL PRESSURE PROFILE CONSTANT β

In the prediction of wind velocity of typhoon, many parameters are involved. Among them, the radius of maximum wind velocity R_{\max} and pressure profile β are two of the most critical parameters.

With the help of WRF-ARW (Advanced Research Weather Research and Forecasting) software which used in simulation of typhoon by Chinese National meteorological center, a new expression of the radius of maximum wind velocity R_{\max} was proposed by Zhao et al (Lu, 2012) as follows

$$E(\ln R_{\max}) = -38.36\Delta P^{0.02479} + 46.75 \quad (27)$$

$$\sigma(R_{\max}) = 10549.2\Delta P^{-1.5178} \quad (28)$$

Where $E()$ denotes average value of $\ln R_{\max}$, $\sigma()$ denotes standard deviation of R_{\max} .

According to comparison research by Zhao et al, the typhoon pressure profile β has a great influence for the results of typhoon-induced wind velocity simulation. Utilizing a large number of on-site observed typhoon data along Chinese coastal regions, a new functional expression of the pressure profile β was proposed (Zhao, et al. 2013) as follows

$$\beta = -2.365 + 0.0573\Delta P + 0.0035R_{\max} \quad (\text{Before landfall}) \quad (29)$$

$$\beta = 0.4899 + 0.0178\Delta P \quad (\text{After landfall}) \quad (30)$$

The above expression is based on the actual pressure data from hundreds of ground stations in Zhejiang province, whether this expression is suitable for other cities located in southeast China coastal areas, more on-site data are needed to verify.

4. COMPARISON OF SIMULATED RESULTS WITH ON-SITE MEASURED DATA

With the help of Xiamen Meteorological Station, 20 typhoon-induced wind velocity series records at the height of 10 m above the ground were obtained. The names, numbers and instantaneous wind velocities of the 20 typhoons are shown in Table1.

Based on Yan Meng typhoon analytical model, using the radius of maximum wind velocity and pressure profile constant expressions in Part 3, the instantaneous wind velocities on the observation site can be simulated. In the simulation, the main

parameters involved are shown in Table 2. Comparison between simulated results and measured results are shown in Figure 1.

Table 1 Measured instantaneous wind velocities of different typhoons

No.	Typhoon Name	Typhoon Number	Instantaneous Wind Velocity
1	Yancy	199012	15.7 m/s
2	Dot	199018	14.7 m/s
3	Gladys	199418	6.3 m/s
4	Tim	199406	14.3 m/s
5	Gloria	199607	13.0 m/s
6	Herb	199608	16.3 m/s
7	Amber	199714	19.0 m/s
8	Dan	199914	5.0 m/s
9	Bilis	200010	14.0 m/s
10	Chebi	200102	7.7 m/s
11	Haitang	200505	10.7 m/s
12	Talim	200513	15.3 m/s
13	Longwang	200519	12.1 m/s
14	Kaemi	200605	12.9 m/s
15	Saomai	200608	5.4 m/s
16	Sepat	200709	13.3 m/s
17	Wipha	200713	8.1 m/s
18	Fung-wong	200808	11.7 m/s
19	Morakot	200908	12.9 m/s
20	Fanapi	201011	15.1 m/s

Table 2 Main parameters in the simulation

Height	longitude	Latitude	Roughness length	Radius of influence	Air density
10 m	118.08°	24.48°	0.05 m(0.01-0.1)	500 km	1.2 kg/m ³

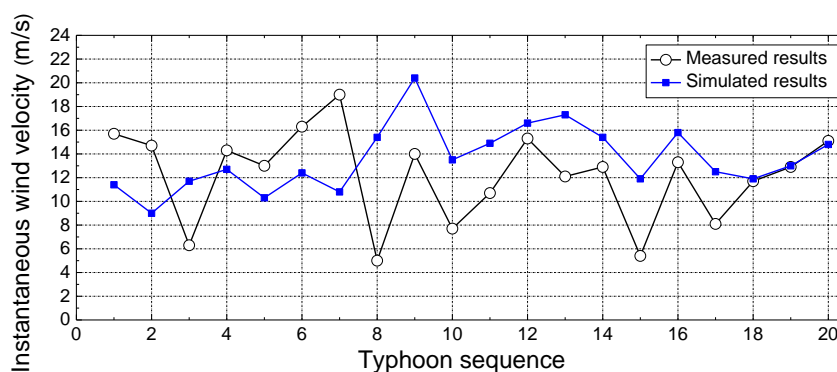


Fig. 1 Comparison between measured and simulated wind velocity

In order to check the validity of the parameters, the error D_{error} is defined to evaluate the simulated results and measured data in Xiamen Meteorological Station.

$$D_{error} = (v_s - v_m) / v_m \quad (31)$$

Where, v_s and v_m are the simulated and measured instantaneous wind velocities respectively. The errors for the 20 typhoon sequences are shown in Figure 2.

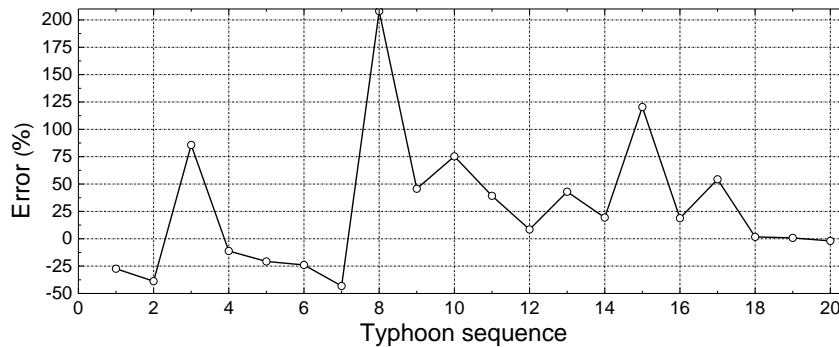


Fig. 2 Comparison between measured and simulated wind velocity

The wind field characteristic difference between different typhoons is very large, which can be obtained from Figure 1 and 2. For typhoon Gladys, Dan, Chebi, Saomai and Wipha, the simulation errors are larger than 50%. On the contrary, in typhoon Tim, Talim, Fung-wong, Morakot and Fanapi, the simulation results are precise and all of the errors are smaller than 11.2%. Especially for typhoon Fung-wong, Morakot and Fanapi, the largest error is just -2%. The mean error of the 20 typhoons is 27.7%. On the whole, in most cases, the simulation method can get a safety typhoon-induced instantaneous wind velocity.

5. CONCLUSIONS

From analysis and comparison of simulated and measured results at Xiamen observation site, 3 conclusions can be obtained as follows,

- (1) The characteristics of wind velocities in typhoon have a great difference between different typhoons.
- (2) Comparison results showed that the expressions of R_{max} and β and the Yan Meng analytical model have great calculation accuracy in the prediction of instantaneous wind velocities of some typhoons in Xiamen, but in some other typhoons the estimation errors are large and the simulated results should be modified.
- (3) More measured wind velocity data of typhoon are needed to check the validity the expressions of R_{max} and β .

ACKNOWLEDGMENTS

The authors gratefully acknowledge the support of the National Natural Science Foundation of China (51508107, 51178353 and 51222809) and Open Project of Key

Laboratory of Wind Resistant Technology in Bridge Engineering of Ministry of Transport (KLWRTBMC14-03).

REFERENCES

- Ge, Y., and Zhao, L. (2014), "Wind-excited stochastic vibration of long-span bridge considering wind field parameters during typhoon landfall", *WIND AND STRUCTURES*, **19**(4), 421-441.
- Holland, G. J. (1980). "An analytic model of the wind and pressure profiles in hurricanes." *Monthly weather review* **108**(8), 1212-1218.
- Lu, A. P. (2012), "Reconstruction of typhoon pressure field and its impact on the design wind velocity for various return periods", *Master Thesis, Tongji University*. (in Chinese)
- Meng, Y., Matsui, M. and Hibi, K. (1995). "An analytical model for simulation of the wind field in a typhoon boundary layer." *Journal of Wind Engineering and Industrial Aerodynamics*, **56**, 291-310.
- Meng, Y., Matsui, M. and Hibi, K. (1997), "A numerical study of the wind field in a typhoon boundary layer", *Journal of Wind Engineering and Industrial Aerodynamics*. **67**, 437-448.
- Ministry of Transport of the People's Republic of China. (2004), "Wind-resistant design specification for highway bridges (JTG/T D60-01-2004)", Beijing: China Communications Press. (in Chinese).
- Ministry of Housing and Urban-Rural Development of the People's Republic of China. (2012), "Load code for the design of building structures (GB 50009-2012)", Beijing, China Architecture and Building Press. (in Chinese)
- Zhao, L., Lu, A.P., Zhu, L.D., Cao S.Y. and Ge, Y.J. (2013), "Radial pressure profile of typhoon field near ground surface observed by distributed meteorologic stations". *Journal of Wind Engineering and Industrial Aerodynamics*, **122**, 105-112.